Egyptian Journal of Aquatic Biology & Fisheries
Zoology Department, Faculty of Science,
Ain Shams University, Cairo, Egypt.
ISSN 1110 – 6131
Vol. 29(1): 997 – 1021 (2025)
www.ejabf.journals.ekb.eg

Sea Surface Conditions of the Milky Sea Phenomenon in the Southern Java Sea: Analysis of SST, Chlorophyll-*a*, and Nutrient Fluctuations

Trisna D. A. Sidik[1,2,3*], Choerunnisa Febriani[1], Muhammad H. Ilmi[1], Fadilla N. Azizah[1], Defania S. Ramadhanti[1], Ghelby M. Faid[1], Ibnu Faizal[2], Marine K. Martasuganda [1], Noir P. Purba[4]

[1]KOMITMEN Research Group, Universitas Padjadjaran, Jatinangor 45363, West Java, Indonesia
[2]Department of Marine Science, Universitas Padjadjaran, Jatinangor 45363, West Java, Indonesia
[3]Master of Marine Conservation Study Program, Universitas Padjadjaran, Jatinangor 45363, West Java, Indonesia
[4]Marine Conservation Department, Universitas Padjadjaran, Jatinangor 45363, West Java, Indonesia
[*]Corresponding Author: trisna20001@mail.unpad.ac.id

ARTICLE INFO

Article History:
Received: Sep. 24, 2024
Accepted: Jan. 14, 2025
Online: Jan. 28, 2025

Keywords:
Milky Sea,
Bioluminescent,
Ocean eddies,
Plankton,
Ocean currents

ABSTRACT

A phenomenon known as 'Milky Sea', an event where marine microorganisms with bioluminescent abilities rising to the surface, has occurred in the southern sea of Java for the first time. This study aimed to analyze the environmental condition during the event. This study used several open portal data, specifically from 30 July 2018, 30 June 2019, and 27 July to 4 August 2019. The results showed the correlation between sea surface temperature (SST) and the concentration of chlorophyll-*a*. The maximum concentration of chlorophyll-*a* was between 0.1-1.5mg/ m^{-3} on August 1st, followed by a decline and a resurgence on August 4th due to the decrease of SST. Several eddy currents and upwelling were discovered in Java's southern sea. However, the coastline section was only visible from 31 July 2019 to 2 August 2019, and faded on 3 August 2019. The ocean current system in the eastern of the Indian Ocean represented key factors in the distribution of chlorophyll-*a* and nutrients colonizing when the Milky Sea occurred. The nutrient concentration, particularly nitrate, fluctuated during the Milky Sea event within a narrow range of 0.01-0.02mmol/ m^3 and showed limited changes. During this time, sea surface temperature (SST) and the concentration of chlorophyll-*a* were associated with the abundance of nanoplankton around the Milky Sea area, which ranged from 0 to 1mg/ m^3. The Milky Sea phenomenon is primarily driven by a decrease in SST and an increase in the concentration of chlorophyll-*a* and nanoplankton, with eddy currents and upwelling acting as catalysts.

INTRODUCTION

Milky Sea in southern Java was first identified in 2019 **(Miller, 2022)**, when the crew of the 16-meter private yacht Ganesha was reported sailing over a shimmering water section on the evening of the 2nd of August 2019. It is a scientific phenomenon in the

ocean caused by biological activity and is extremely rare. A milky-white color with a fairly uniform luminescence is circumnavigating the ship after 15 minutes of steaming. The Operational Linescan System (OLS) of the Defense Meteorological Satellite Program (DMSP) later confirmed from space that the S.S. Lima had traveled 90km from shore in the ocean of Bima, where a bright, comma-shaped zone of 15,400km^2 could be seen on OLS imagery. The shimmering ocean swath remained for several nights in a row, progressively encircling a cold-core eddy's eastern edge **(Miller *et al.*, 2021)**. Previous research has stated that the Milky Sea occurs due to the presence of marine bioluminescent organisms **(Wibowo, 2021)**. There are numerous marine creatures, including fungi, bacteria, plankton, algae, and others that are capable of bioluminescence **(Miller *et al.*, 2005)**. Moreover, there are several impacts resulting from the milky sea phenomenon, particularly from bioluminescent microorganisms **(Haddock *et al.*, 2010)**. The bioluminescent microorganisms involved can affect the food chain, population dynamics, and behavior of marine animals. Socially, the phenomenon has a positive effect on tourism and ecotourism, attracting many visitors who want to witness the glow of the sea. Scientifically, bioluminescence serves as a "danger marker" that attracts larger predators when the light is triggered by contact with a predator **(Mesinger & Case, 1992)**.

More than 70% (171 cases) of the reported Milky Seas occurred in the northwestern part of the Indian Ocean, mainly in summer during the southwest monsoon. There is also a small group (about 17%) that occurs in the waters around Java, Indonesia **(Miller *et al.*, 2005)**. Bioluminescence organisms have been identified in several locations including the South Sea of Java in 2019. The Milky Sea is most commonly reported in the northwestern Indian Ocean region and in the waters around Indonesia. This area is known for having deep upwelling conditions, high primary production, and warm sea surface temperatures (SST). A commonality noted in ship reports is the presence of a wide and constant spread of light in the absence of mechanical stimuli, such as breaking waves or ship waves **(Miller *et al.*, 2021)**. By understanding the anomaly of environmental conditions during the Milky Sea phenomenon, the presence of the Milky Sea phenomenon can be modeled for future research.

Based on oxygen and nutrient levels, the oceanographic conditions in the Indian Ocean reveal that the water masses in the upper and lower layers are distinct. The uppermost water mass contains a relatively thick oxygen layer and is rich in nutrients **(Purba *et al.*, 2025)**. Water mass in the southern Indian Ocean has a strong nutrient content and it is rich in nutrients **(Sardessai *et al.*, 2010)**. The eastern Indian Ocean mass water was also affected by Indonesia Throughflow (ITF), especially in the South of the Java Sea. The ITF caused an anomaly in SST and salinity values. The ITF transport appears seasonally with maximum SST and salinity values in July-September **(Qasim, 1999)**. The eastern part of the Indian Ocean, including the South Sea of Java, is affected

by El Niño Southern Oscillation (ENSO) and the Indian Ocean Dipole (IOD) phenomenon that caused anomalies in oceanographic conditions.

The South Sea of Java has a unique oceanographic dynamic, as the land affects the Indian Ocean climatologically by causing seasonal monsoon cycles. The monsoon cycle generates seasonal currents on the South Coast of Java, namely the South Java Current (SJC) **(Purba *et al.*, 2018)**. The SJC has an important role in the circulation of water masses and heats the southern-eastern boundary of the Indian Ocean. Another impact of the monsoon cycle in the South Java Sea is the occurrence of upwelling phenomena along the coast of the southern waters of Java. Monsoon winds generate the upwelling phenomenon and create Ekman Transport (EMT). This condition must be studied further by the researcher. Therefore, this study aimed to model the oceanographic and environmental conditions as factors in the presence of the Milky Sea in the South of Java in 2019.

MATERIALS AND METHODS

1. Study area

The observed area was the eastern part of the Indian Ocean (EIO), more detailed in the area near the southern part of Java with coordinates 6.5582°S – 105.6176°E and 14.2704°S – 115.6909°E. The circulation of water in the eastern part of the Indian Ocean is influenced by the annual monsoon cycle, which influences the physical oceanographic characteristics of the waters, such as SST and ocean current (Fig.1). The enrichment in the waters is also influenced by the annual monsoon cycle.

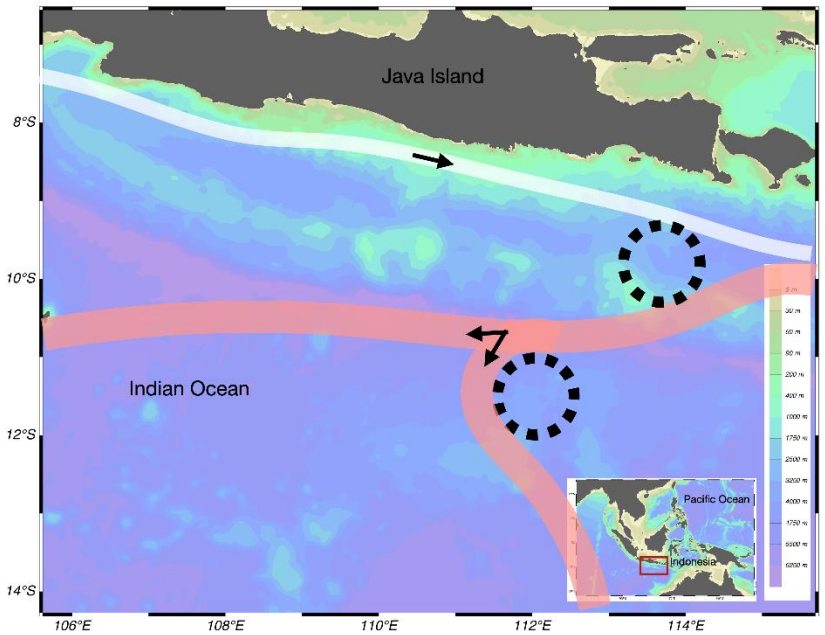

Fig. 1. A Map of the Study Area in eastern Indian Ocean near the Southern Part of Java with current system and circulation adapted from several authors **(Purba *et al.*, 2018;**

Ahmad *et al.*, 2019; Auer *et al.*, 2019; Khan *et al.*, 2024) The white arrow represents South Java Current (SJC), the black arrow represents eddies, and the orange arrow represents Indonesia Throughflow (ITF)

The currents in the southern waters of Java are influenced by ENSO and the IOD phenomena. Both phenomena will affect changes in seawater temperature during El Niño and La Niña events and will affect the intensity of upwelling **(Setiawan *et al.*, 2015; Purba & Khan, 2019)**. In December-March, the wind blows to the northwest, as well as when entering June – October, the wind blows to the southeast **(Purba *et al.*, 2021)**. High-intensity upwelling occurs during El Niño, which is associated with the southeast monsoon and decreases in intensity during La Niña, which is associated with the northwest monsoon. Upon the occurrence of upwelling, it is characterized by a decrease in temperature, an increase in salinity, and an increase in the number of nutrients at the surface, which has an impact on water fertility and primary productivity **(Atmadipoera *et al.*, 2020)**.

The eastern part of the Indian Ocean, including the southern waters of Java, experiences ocean currents influenced by both remote forcing from the equatorial area and local impacts. The ocean current is influenced by ocean-atmosphere interactions such as ITF, ENSO, and IOD. This interaction causes upwelling and eddies current in this area. This study area was also affected by current systems, such as SJC, SEC, and EGC. ITF, which pass through this area and supply warm water to the Indian Ocean from the Pacific Ocean; the SEC contributes to the internal circulation of ITF. This study was carried out using the secondary data analysis method based on data taken from the global marine data portal. Some of the data parameters downloaded to detect the Milky Sea were SST, chlorophyll-*a* (Chlor-*a*), nutrients, plankton, and ocean current.

2. Data sources

The observation period was selected to be twelve days from 30th July 2018, 30th June 2018, and 27th July – 5th August 2019. This period was used to compare the range parameters in normal conditions, pre-milky sea conditions, and when the Milky Sea occurred. In this study, we focused on primary and secondary parameters to detect Milky Sea, which are SST, Chlor-*a*, nutrients, plankton, and ocean current. The data used were obtained from NASA Ocean Color (https://oceancolor.gsfc.nasa.gov/), Marine Copernicus (https://data.marine.copernicus.eu/) and ERDDAP National Oceanic and Atmospheric Administration (https://coastwatch.pfeg.noaa.gov/erddap/) global portal data (Table 1).

SST was collected from AQUA-Modis satellite data with spatial resolutions of approximately 4km; the day and night SST data were collected to compare the differences of SST in the daytime with the Milky Sea that occurred in the nighttime **(NASA Ocean Biology Processing Group, 2024)**. Chlor-*a* and plankton data were obtained from Global Ocean Color and Reflectance MY L3 Daily **(CMEMS, 2023)**. Data

were collected from multi-satellite observations, namely SeaWiFS, MODIS, MERIS, VIIRS-SNPP, OLCI-S3A & OLCI-S3B, with spatial resolutions of about 4km and daily temporal resolution. The data were in near real time (NRT) and long time series (from 1997) in datasets called Multi-Years (MY). Ocean current data were collected from NOAA satellite observation in near real time geostrophic current gridded datasets with dataset ID name Miami current **(ERDDAP, 2023)**; the data were on a near-real-time basis with two-days average delay and corresponding to 10-days period ending on the selected date. Nutrient data, specifically nitrate concentrations, were obtained from the Global Ocean Biogeochemistry Hindcast dataset with Level 4 (L4) resolution and a spatial resolution of 0.25° × 0.25°. The data were modeled using the PISCES biogeochemical model, implemented on the NEMO modeling platform version 3.6. **(CMEMS**, **2023)**.

Table 1. Data sources for modeling

No.	Data name	Variable	Resolution		Data type
			Temporal	Spatial	
1.	AQUA-Modis Sea Surface Temperature (L3) (11 Daytime) and (4 Night time)	SST	Daily	4 × 4 km	Ocean Colour
2.	Global Ocean Color and Reflectances MY L3	Plankton	Daily	4 × 4 km	Ocean Colour
3.	Global Ocean Color and Reflectances MY L3	Chlor-a	Daily	4 × 4 km	Ocean Colour
4.	Global Ocean Biogeochemistry Hindcast	Nutrient	Daily	0.25° × 0.25°	Hindcast
5.	Near Real Time Geostrophic Current	Ocean Current	Daily	0.25° × 0.25°	Gridded

3. Analysis

The collected data from NASA Ocean Color (https://oceancolor.gsfc.nasa.gov/), Marine Copernicus (https://data.marine.copernicus.eu/) and ERDDAP National Oceanic and Atmospheric Administration (https://coastwatch.pfeg.noaa.gov/erddap/) global portal data included SST, Chlor-*a*, nutrient, plankton and ocean current. SST and Chlor-a were selected as the primary parameters, as previous studies regarding milky seas have identified them as key factors contributing to their occurrence **(Miller *et al.*, 2021)**. The secondary parameters were utilized to support the result of the primary data. The data were then processed and analyzed using the Ocean Data View (ODV) software. The data were interpolated using a weighted-average gridding interpolation method, applied to scalar values and XBT/MBT corrections.

Estimates $c_e = \frac{\sum_i a_i \cdot d_i}{\sum_i a_i}$ where $a_i = e^{-r}$ with $r = \left(\frac{\Delta x}{L_x}\right)^2 + \left(\frac{\Delta y}{L_y}\right)^2$

Weighted-average gridding converts scattered or irregularly spaced data points into a regular grid format, where each grid cell is assigned a value based on the weighted

average of nearby data points. The algorithm fills gaps between data points and provides estimates for unsampled locations, ensuring uniform data coverage. To visualize the parameters on the grid, different color palettes were applied: the Ferret blue-orange palette for SST, the Crameri Imola pallet for dissolved oxygen, the Matplotlib plasma pallet for nitrate, and the Matlab parula pallet for Chlor-*a*, The grids utilize color management to organize data across both time and space. Additionally, current data processed in ODV software were overlaid with SST, Chlor-*a*, nitrate, and nanoplankton data for comprehensive analysis. Four stations of satellite observation data were used around the Milky Sea area. Data taken from satellite observation stations were statistically processed with Excel 2019 (Table 2). The results of the data visualization were then analyzed with the descriptive quantitative method to determine the correlation between parameters and the Milky Sea phenomenon.

Table 2. Statistical analysis

Parameter	Max	Min	Mean	Sta.dev	Sta.err
SST Night (℃)	28.205	19.135	25.298	0.927	0.007
SST Day (℃)	31.485	22.080	25.681	0.762	0.005
Chlorophyll-*a* (mg/m^{-3})	20.753	0.089	0.550	0.560	0.001
Nitrate (mmol/m^{-3})	0.089	0.001	0.789	1.571	0.013
Nanoplankton (mg/m-3)	0.64	0.02	0.216	0.114	0.0002

RESULTS AND DISCUSSION

1. SST condition

The condition of SST around the southern waters of Java during this period (Fig. 2) was relatively homogenous with a range of 25 – 27℃; this average value of SST was in accordance with research conducted in 2020 **(Sofiati *et al.*, 2020)**. The value of SST in the southern waters of Java is also influenced by water masses from the Pacific Ocean and Western Indian Ocean, which were brought by ITF. The movement of water mass caused by the difference in height between the Pacific Ocean and the eastern Indian Ocean caused a current flow **(Herwindya *et al.*, 2018)**.

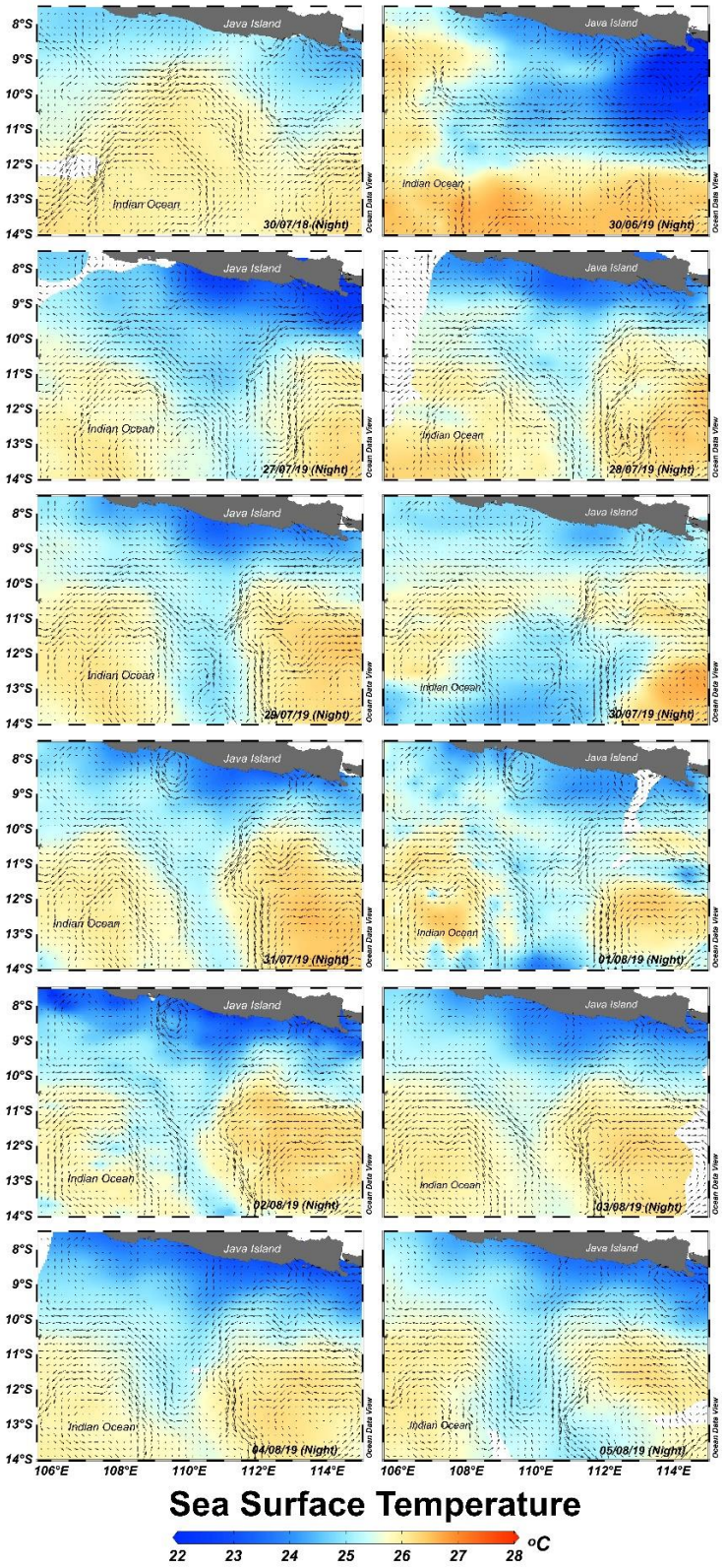

Fig. 2. Night sea surface temperature combined with surface currents in EIO from 30 July 2018, 30 June, and 27 July – 4 August 2019

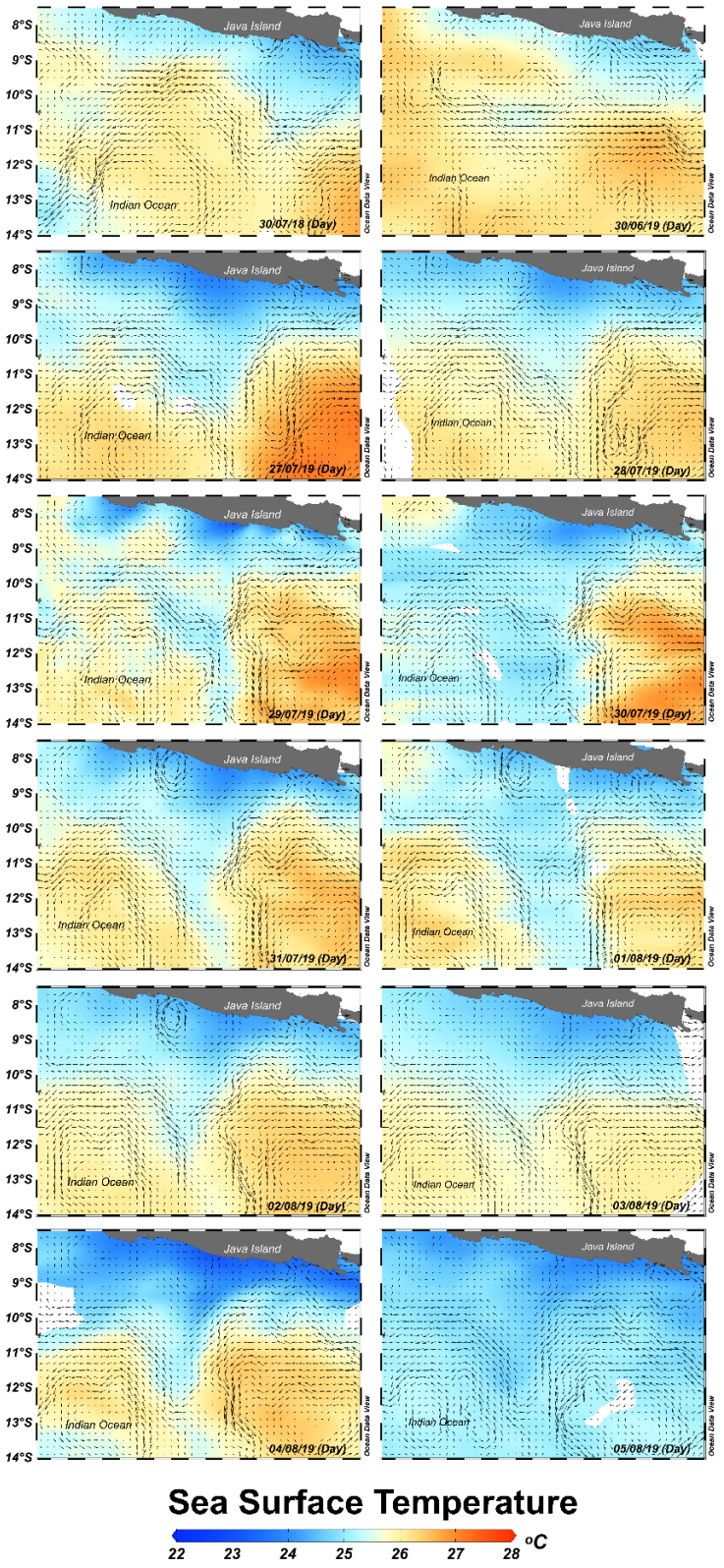

Fig. 3. Day sea surface temperature combined with surface currents in EIO from 30 July 2018, 30 June, and 27 July – 4 August 2019

Based on the results in Figs. (2, 3), on the 30th of July 2018 and the 30th of June 2019, the EIO waters were still in normal conditions with SST distribution in the coastal part lower than the high seas. Prior to the occurrence of the Milky Sea from 27 July to 30 July 2019, the water condition showed variations in the distribution of SST, during both day and night. During this period, the formation of the Milky Sea area was observed, although on some days, the formation was incomplete. Ocean surface current has affected migration of the colonizing microorganism that wrapped around the eddies, the spreading of mass water and SST. SST value around the study area was warmer because there has not been much upwelling, and it showed that eddies were forming.

During two days (31st July to 1st August 2019), the eddies were fully formed and a lot of upwelling patterns were seen. The distribution of SST value around the study area was increased but not too significant when the Milky Sea was reported on the 2nd of August 2019 and became cooler until the 4th of August 2019 since the eddies and upwelling started to spread, bringing water masses from another area **(Sofiati *et al.*, 2020)** and faded on the 5th of August 2019. The occurrence of the Milky Sea at night is more visible than during the day (Fig. 2) because the SST value during the day tends to be warmer. Day and night conditions did not experience significant differences when the Milky Sea phenomenon occurred.

The cooler SST value was seen on the coast of South Java, around the eddies area, with a range of 22 – 23.5°C. The area where the Milky Sea occurred was in 110 – 111°E and 9 – 14°S. During the Milky Sea event (night), the SST values in the waters exhibited a narrow range and were relatively low, with a maximum temperature of 25 ± 1°C **(Miller *et al.*, 2021)**. Upwelling was predominantly found in coastal areas, where the ocean's current direction appears to be heading toward the Indian Ocean, away from the coastal area, and creating boundaries between eddies. This resulted in the distribution of SST values extending southward into the Indian Ocean, forming an inverted triangle similar to an anvil (Fig. 2). The area size, where the Milky Sea occurred during five days (31st July until 4th August 2019), was approximately 50.000 – 10.000km^2 **(Miller *et al.*, 2021)**.

The minimum SST value occurs at night, while the maximum SST value occurs during the day (Table 3). This occurrence happened due to the positive IOD in mid-2019. The positive IOD itself is in charge of waters that tend to be warm with strong winds from east to west, thus generating upwelling **(Saji *et al.*, 1999)**. The most frequent occurrence of upwelling is found at night.

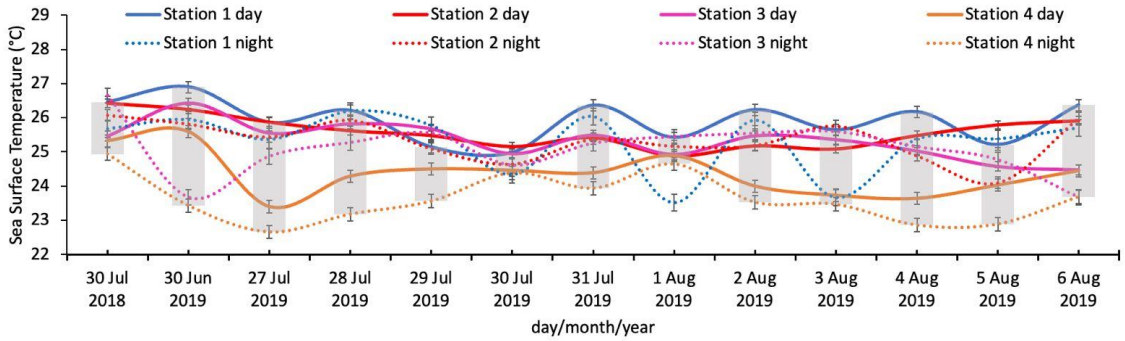

Fig. 4. Sea surface temperature value, day and night per station, from 30 July 2018, 30 June, and 27 July – 4 August 2019

According to the graph, the highest SST value was 26.90℃ at Station 1 during the daytime on 30th of June 2019, while at Station 3 during the night time, the SST value reached 26.65℃ on 30th of June 2018. The lowest SST value is seen in the graph of Station 4 at night, where the SST figure begins to decline before the Milky Sea and continues to fluctuate until the end of the Milky Sea phenomenon (Fig. 4). Station 4, located closest to the South Coast of Java has low SST values during this period, which can be contributed to frequent upwelling from July to October, with peak upwelling in August and September. Over the past three decades (1982-2015), the waters in this region were also warmed at a much lower rate than adjacent ocean locations **(Varela *et al.*, 2016)**.

The coastal upwelling in the South Jave Sea is caused by wind, which can be hypothesized as water mass flux that is moved offshore by wind stress from the coastal upward flow of colder water **(Naulita *et al.*, 2020)**. Although the sea surface temperature (SST) values are fairly homogeneous within the daily range, they fluctuate within the seasonal range. These fluctuations in SST are influenced by the monsoon cycle. During this period, monsoon winds generally blow from the East to the Southeast from April to October each year. Upwelling along the south coast of Java occurs through the advection process, where heat is transferred from the water to the atmosphere by wind. From June to August, this advection process is particularly affected by the Southeast Monsoon **(Kunarso *et al.*, 2011)**. It has been mentioned previously that water mass influences the distribution of SST; in the southern waters of Java, the water mass transport is not only caused by ITF but also due to zonal wind and the SEC, which increase the intensity of upwelling on the southern coast of East Java **(Wyrtki, 1962)**.

The SST value around the Indian Ocean in 2019 was warmer than that occurred in 2018. IOD and ENSO interact with upwelling because they play an important role in the hydrological cycle on the southern waters of Java. In 2019, the Indian Ocean experienced an extremely positive IOD, causing drought in Indonesia and a change in SST anomalies **(Wang *et al.*, 2020)**. In July, IOD intensified and reached its peak in November, but the anomaly of SST was slightly above normal and the ENSO decreased to zero when it

came to September **(Ratna *et al.*, 2021)**. The IOD and ENSO do not significantly affect SST in the study area, and their impact was likely moderated by another local factor, such as the monsoon cycle. This supports the result of previous research conducted by **Haryanto *et al.* (2021)**.

2. Chlorophyll-*a*

Chlor-*a* concentration is closely correlated with SST; the distribution patterns of Chlor-*a* and SST are directly proportional. When the SST gets colder, the Chlor-a concentration gets higher. During this period, the distribution of Chlor-a formed like an anvil. By tracking the spread of Chlor-*a*, the occurrence of the Milky Sea can be identified. The Chlor-*a* concentration, which is derived from satellite observations, is commonly used as a proxy of the plankton in the surface waters but does not provide any information about which plankton group dominates. In this period, Chlor-*a* concentrations were increased especially when the SST became cooler. In Fig. (5), the visualization of Chlor-a has a similar structure to the Milky Sea in South Java waters, reported in the study of **Miller *et al.* (2021)**. The correlation between Chlor-*a* concentration and SST indicates that when the SST becomes cooler, it impacts the increase of Chlor-*a* value in the range of 0.5 – 4mg/ m^{-3}. The highest concentration of Chlor-*a* in the study area was primarily found near the coastal areas and was marked with a bright yellow color. The concentration of Chlor-*a* is strongly influenced by the nutrient inputs from the land, which are then distributed by ocean currents.

The distribution of Chlor-*a* and SST in the southern Java Sea is influenced by the surrounding ocean currents. This region is affected by upwelling and eddies, especially when the Milky Sea occurs. The eddies were formed due to differences in pressure and the Coriolis effect **(Sabhan *et al.*, 2020)**. As shown in Figs. (2, 3, 5) numerous anticyclone eddies were discovered, often triggered by anomalies in sea level height and sea temperature. A significant number of eddies and upwelling were observed between 30 July and 4 August 2019 around the Milky Sea area, occurring at 110 – 111°E and 9 – 14°S (Figs. 2, 3). When the eddies and upwelling occurred, there were mixing and replacement of the water column between the surface and the bottom layer, causing the Chlor-*a*, along with nutrients, to be lifted to the surface as the base of the oceanic food chain. The correlation between upwelling and concentration of Chlor-*a* is largely driven by nutrients such as nitrate (NO_3), rising to the surface and resulting in an increase in Chlor-*a* concentration **(Wei *et al.*, 2012)**.

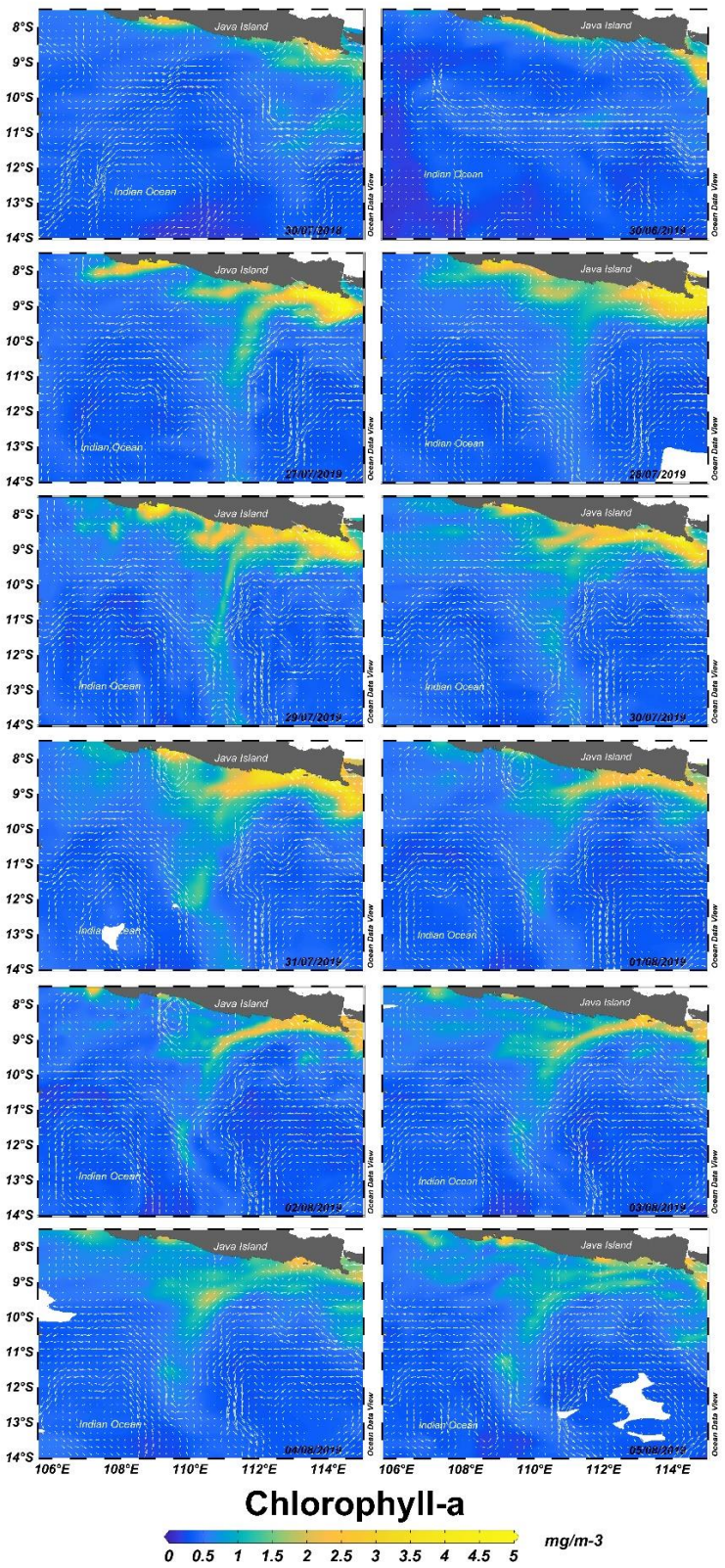

Fig. 5. Daily chlorophyll-a combined with surface currents in EIO from July 30, 2018, June 30, and 27 July – 4 August 2019

Based on Chlor-*a* data from the four stations, the value of Chlor-*a* concentration at Station 4 exhibited a significant increase in concentration, reaching 3.45mg/ m^{-3} (Fig. 6). Chlor-*a* concentration at Station 4 has the highest average concentration compared to the other three stations; this can occur due to its proximity to the coast and is influenced by input from the land. However, on 31 July 2019, when the Milky Sea phenomenon began, the Chlor-*a* concentrations at Stations 1, 3, and 4 were approximately the same. This pattern also occurred on the 2nd and 3rd of August 2019 with a Chlor-*a* concentration value ranging from 0.5 – 0.8mg/ m^{-3}. Whereas, on the 1st of August 2019, only Stations 2 and 4 showed an increase in Chlor-*a*, which was marked by a more intense yellow color at their coordinates. While, the other two stations had approximately the same value as the previous day period.

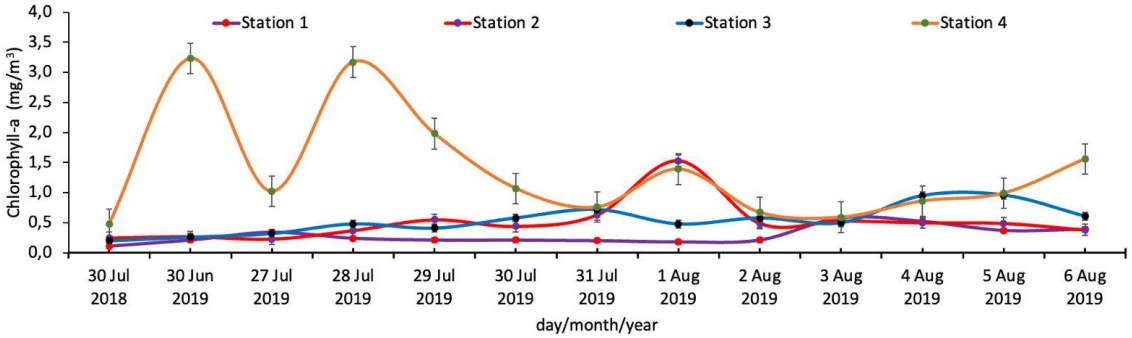

Fig. 6. Chlorophyll-*a* value per station from 30 July 2018, 30 June, and 27 July – 4 August 2019

According to Table (3), the highest value of Chlor-*a* was 20.753mg/ $m^{-3,}$ and the lowest was 0.089mg/ m^{-3}. During this period, eddies enter the eastern season, which results in the formation of well-developed eddies. The ocean current pattern in the eastern Indian Ocean greatly influences the occurrence of these eddies. The upwelling phenomenon is caused by the differences in mass water in the southern sea of Java water, which is affected by SJC, SEC, and ITF. In addition to these water mass differences, eddies and upwelling phenomena in the southern sea of Java during this period were also influenced by ITF flows, whereas in the east season, the intensity of the ITF is relatively high **(Pranowo *et al.*, 2016)**.

Monsoon were also correlated with the concentration of Chlor-*a*, as the monsoon winds induce strong mixing processes that lead to upwelling in the study area **(Wisetya Dewi *et al.*, 2020)**. SST and Chlor-*a* are key parameters in the detection of the Milky Sea phenomenon, supported by the fact that the Milky Sea occurs in the eastern monsoon season when significant upwelling brings nutrient-rich, cold deep-sea water to the surface and fosters abundant biomass. Similar research on the Milky Sea in the northwestern Indian Ocean has identified SST and Chlor-*a* as the primary variables for detecting the event. Ocean currents also play a crucial role in maintaining the shape, direction, and size of the Milky Sea **(Miller *et al.*, 2021)**.

3. Nitrate

In the study area, nitrate levels were found in areas around the coast and shallow waters. Based on Government Regulation No.20/1990 and the Ministry of Health Regulation No.416/1990, nitrate levels in normal waters should not exceed 10mg/ L or about 312mmol/ m^{-3} **(Amalia *et al.*, 2021)**. In general, normal nitrate levels in waters based on each layer range from 0 – 4mg/ L, or about 0 – 124,8mmol/ m^{-3} **(Arizuna *et al.*, 2014)**. Milky Sea occurs due to bioluminescence from marine microorganisms, namely dinoflagellates. Nutrient content affects the abundance of dinoflagellates in the waters, where higher dinoflagellate abundance is found in nutrient-rich environments. One of the nutrients that indicate the abundance of dinoflagellates is nitrate. High nitrate content is utilized by dinoflagellates to carry out photosynthesis. Nitrate is then found in the surface layer during the primary productivity process **(Pratiwi *et al.*, 2015)**.

On 30 July 2018 and 30 June 2019, areas that have high nitrate values are in the coastal region from 8 – 10°S, with no significant changes observed in the range of 0 – 5mmol/ m^{-3}. On 27 July 2019, nitrate distribution began to form and increased in the area located at 9°S, 112°E from 28 July to 4 August 2019, characterized by increase in nitrate levels from a range of 0 – 6mmol/ m^{-3} (Fig. 7). This indicates that the study area is categorized as having low nutrient level but still within quality standards due to the influence of low Chlor-a concentrations, which range from 0.1 – 0.5mg/ m^{-3} **(Rasyid, 2016)**. The highest Chlor-a concentration in the eastern affects the intensity of bacterial bioluminescence. The higher level of Chlor-a, causes the lower the presence of bacteria that cause milky seas, and vice versa **(Serodja *et al.*, 2023)**.

This study period occurred in the east monsoon season when the wind moves eastward, affecting the distribution of nutrients in the sea. This is due to temperature changes that affect upwelling patterns, causing nutrients such as nitrate to rise to the surface. The distribution of nitrate in the waters can be influenced by ocean circulation, which is driven by sea surface currents **(Paringgi, 2019)**. These currents are affected by tides. A high concentration of nitrate can occur during low tide. At high tide, the mixing of seawater with river water increases salinity, causing lower nitrate concentrations than at low tide **(Sumantra *et al.*, 2020)**. On 27 July – 5 August 2019, the lowest tide occurred in the morning around 05.00 – 10.00, while the highest tide occurred in the afternoon around 16.00 – 18.00, but it receded again at night around 21.00 – 24.00. As the day progresses, tide levels tend to rise due to seasonal influences **(Rosel & Mullin, 2011)**. This phenomenon is related to the Milky Sea event, which generally occurs at night.

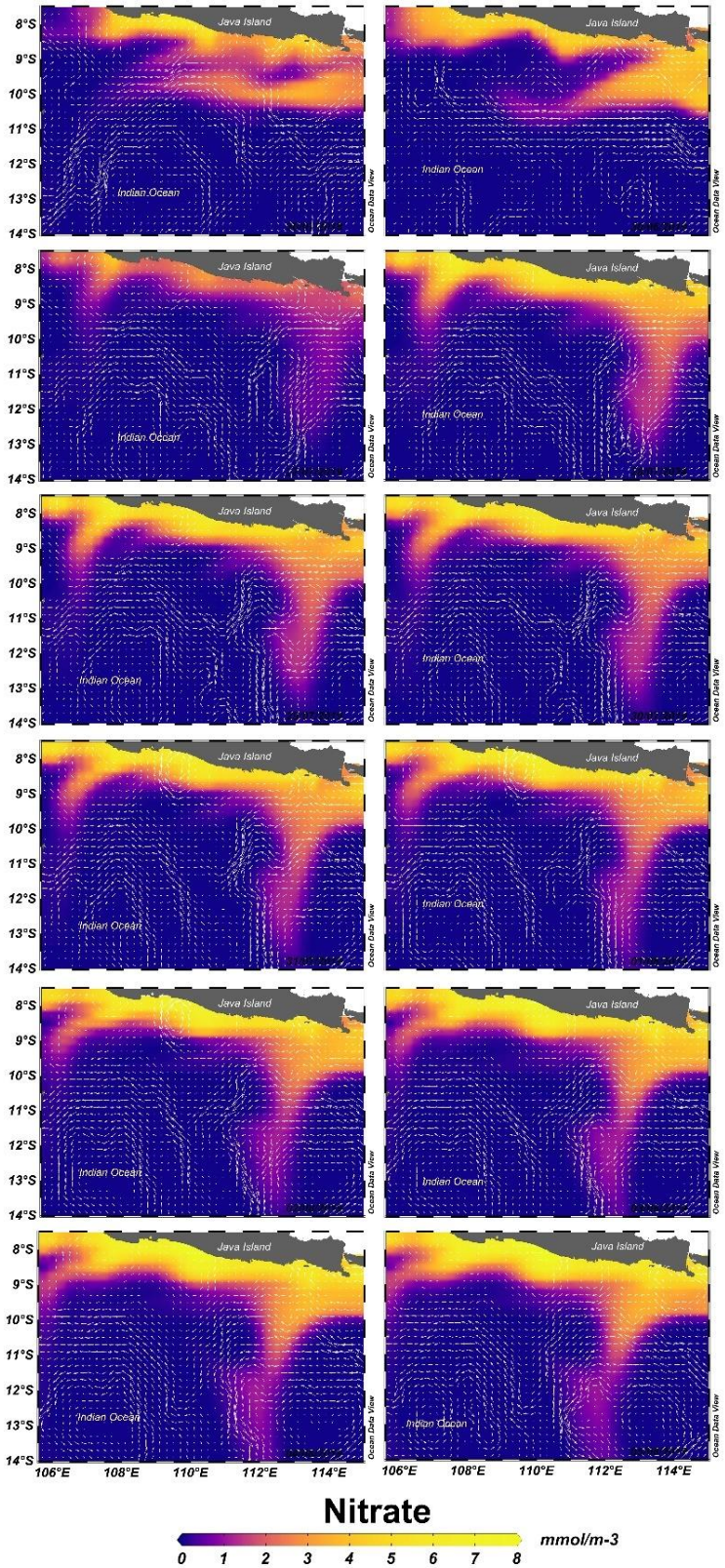

Fig. 7. Daily visualized nitrate combined with surface currents in EIO from 30 July 2018, 30 June, and 27 July – 4 August 2019

The graph shows the highest and fluctuating nitrate values at Station 4, located at 8°S and 110°E. Station 3 had only a single value of 0.9mmol/ m^{-3} on 30 July 2018, with no value shown the following day. Meanwhile, Stations 1 and 2 have no nitrate values at all, so the graph forms a straight line (Fig. 8). The high nitrate value at Station 4 was influenced by inputs from the land through the river estuary, causing waste and feed residue to be decomposed by bacteria into nutrients **(Patty, 2015)**. Based on the Table (5), the highest value of nitrate was 8.951mmol/ m^{-3}.

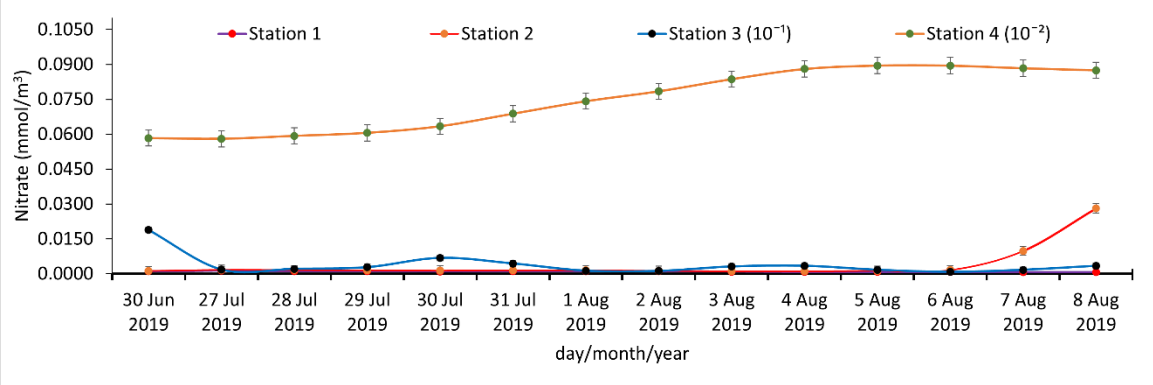

Fig. 8. Nitrate fluctuation in each station Station from30 June 2019 and 27 July – 4 August 2019

Based on the correlation between SST and nitrate distribution, the temperature that occurred between 30 July 2018 and 30 June 2019 did not change significantly. This is due to that the SST in that period was relatively low. However, on 27 July 2019, there was an increase in temperature, which affected the nitrate values in the waters. This indicated that nitrate levels in the waters would peak at the highest temperature during the time period from 28 July – 5 August 2019. On 5 August, nitrate levels in the water returned to normal, coinciding with a decrease in SST. Based on the graph of nitrate value correlated to SST and Chlor-*a* graph, the relationship can't be defined. This can occur because the data on nitrate are biased. This statement identified by the value of nitrate concentration only appears on station 4; meanwhile, other stations values are mostly near zero.

Nutrient substances needed by phytoplankton, especially nitrate, can affect the Chlor-*a* content contained in phytoplankton **(Hackett *et al.*, 2004)**. The maximum nitrate levels occur in coastal areas, while the minimum nitrate levels occur when moving away from the coast toward the open sea (Table 3). This confirms that in coastal areas, there is a terrestrial influence that can affect nitrate levels. Based on the results, the highest nitrate value is at station 4, where the area is still in the coastal area instead of where the Milky Sea occurs; the correlation between nutrients which is an indication of the presence of dinoflagellates as a catalyst for the milky sea still needs further research. The positive relationship of Chlor-a, nitrate, and SST leads to the possibility of fishing zones due to the nutrient-rich water condition that is also stimulated by the upwelling around this study area **(Zainuddin *et al.*, 2017)**.

4. Nanoplankton

Dinoflagellates are responsible for most of the bioluminescence in the surface ocean, producing a small, fleeting flash of light that lasts less than 0.1 seconds and yet is roughly ten times brighter than luminous bacteria **(Miller**, **2022)**. In both freshwater and marine environments, dinoflagellates comprise a significant group of phytoplankton that is classified under the division Pyrrophyta and class Dinophyceae **(Neliyana *et al.*, 2016)**. Phytoplankton abundance in water can be measured by the concentration of Chlor-*a*. The pigment in Chlor-*a* is one of the most dominant in phytoplankton and plays a role in carrying out the photosynthesis process **(Valiadi & Iglesias-Rodriguez, 2013)**. The distribution of SST can be related to the phenomenon of upwelling, where colder water masses from lower layers rise to the surface, resulting in lower surface temperatures and a higher level of fertility **(Yan *et al.*, 2023)**.

In some cases, the Milky Sea occurred because of the representation of dinoflagellates and bacteria of the genus *Vibrio* **(Miller *et al.*, 2006)**. Dinoflagellates may be present in nanoplankton that are planktonic organisms with 2-20µm size; the other species of dinoflagellates could be bigger or smaller **(Valiadi Iglesias-Rodriguez, 2013)**. Dinoflagellates are capable of producing light and are primary eukaryotic protists **(Yan *et al.*, 2023)**. The dinoflagellate abundance is significantly and positively correlated with temperature and negatively associated with nutrients, which indicates that temperature affects dinoflagellate growth. However, dinoflagellate can thrive better in nutrient-deficient environments **(Fischer *et al.*, 2020)**. Fig. (6) shows that the concentration of nanoplankton around the study area follows the same pattern as SST at night and Chlor-a levels. From 27th July 2019 until 5th of August 2019, at 110 – 111°E and 9 – 14°S (Figs. 2, 3), the concentration remained within a range of 0.3 – 0.7mg/ m^{-3}.

Ocean current patterns can affect the growth and migration of microorganisms, including dinoflagellates that can cause the Milky Sea. Ocean currents can carry microorganisms from various locations to a specific area, influencing the emergence of the Milky Sea on a certain time scale. There are several eddy currents that occur in the southern water of Java. However, eddies along the southern coast of Java were only visible from 31st of July to 2nd of August 2019 and began to fade on 3rd of August 2019. In addition to eddies, there is a significant upwelling around the Milky Sea area. Warm surface temperatures and upwelled nutrients help fuel nanoplankton growth. Stratification of the water column is usually beneficial for dinoflagellate growth, although dinoflagellate abundance can decrease due to increasing upwelling **(Fischer *et al.*, 2020)**. As a result of upwelling, water temperatures fell while wind shifts caused the seafront to move shoreward at a velocity of at least several miles per hour **(Pitcher *et al.*, 1998)**. In response to downwelling or upwelling-favorable winds, surface currents frictional layer tend to migrate onshore or offshore relative to the direction of the mean current **(Trainer *et al.*, 2009)**.

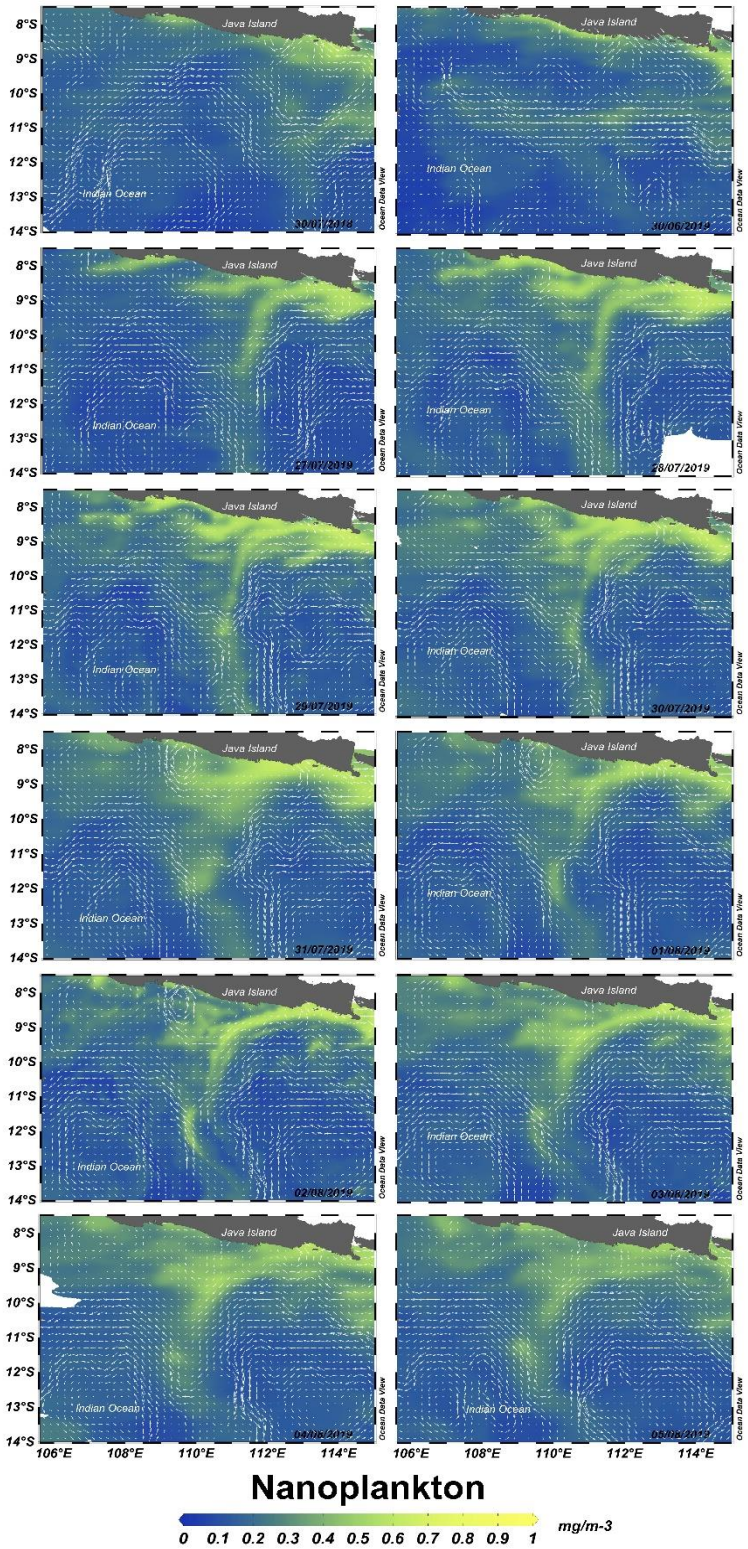

Fig. 9. Daily visualized nano-plankton combined with surface currents in EIO from 30 July 2018, 30 June, and 27 July – 4 August 2019

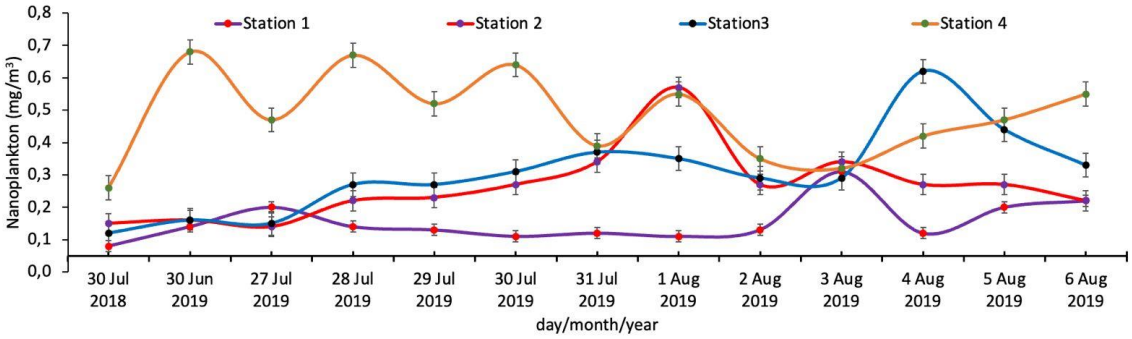

Fig. 10. Nanoplankton value per Station from 30 July 2018, 30 June, and 27 July – 4 August 2019

Based on the graph, the nanoplankton value at Station 4 was relatively high compared to the other 4 stations, with the highest nanoplankton value around 0.7mg/ m^{-3} on 30 June 2019. Station 3 reached its peak on 4 August 2019, compared to the previous days, but then decreased again until 8 August 2019. The graph shows the intersection among multiple stations, such as Station 2 with 3 on 30 June 2019 with a value of 0.11, and Station 1 with 2 on 6 August 2019 with a value of 0.17mg/ m^{-3}. The lowest nanoplankton value was at station 1 on 30 July 2018 (Fig. 10). According to Table (3), nanoplankton has a maximum value in coastal areas, while it has a minimum value in the open sea. The abundance of nanoplankton can be influenced by upwelling that occurs in coastal areas. Upwelling can significantly affect nanoplankton by bringing nutrient-rich water to the surface, which simulates the growth of phytoplankton, including nanoplankton **(Böttjer & Morales, 2007)**. Nanoplankton are essential in fisheries as they contribute to ecosystem biomass and regulate bacterial populations, which helps to maintain the balance of aquatic ecosystems and makes them vital for the sustainability of fisheries **(Das & Pandey, 2015)**.

The amount of nanoplankton in the oceans was influenced by both SST and Chlor-a levels; when SST was too high, the concentration of nanoplankton decreased. Nanoplankton have a positive relationship with nutrients and Chlor-a; they grow abundantly in water with high nutrients, and their abundance is highly proportional to Chlor-a concentration (Figs. 5, 7). It is because nanoplankton contains Chlor-a pigments in its body for photosynthesis **(Khan *et al.*, 2024)**. The contribution of nanoplankton to Chlor-a value in the water ranged from 7 to 73%, indicating a considerable concentration **(Hirata *et al.*, 2011)**. Although this range of variation in the contribution is smaller than micro and picoplankton, it means that nanoplankton was likely to have a more consistent contribution to the total Chlor-a value in the ocean.

CONCLUSION

Oceanographic conditions that occur in the eastern Indian Ocean are influenced by several atmospheric interactions, such as the ITF, ENSO, and IOD. The SST value during

the Milky Sea was between 22 – 23.5℃. This shows that the Milky Sea tends to occur when the SST is low, especially during the night. The Milky Sea phenomenon began to form between July 27th and 30th in 2019, and fully developed over the course of five days (July 31st to August 4th, 2019), before starting to decrease on August 5th, 2019. The area affected by the Milky Sea spanned approximately 50,000–10,000km^2. Key factors such as chlorophyll-*a* (Chlor-a), sea surface temperature (SST), ocean currents, upwelling, and eddies interact with each other in the southern waters of Java.

Chlor-a concentration increased within a range of 0.089 – 20.753mg/ m^3 due to a decrease in SST. This reduction in temperature supports Chlor-*a* growth, particularly during upwelling patterns. Upwelling and eddies in this region are also influenced by the strong flow of the Indonesian Throughflow (ITF). The nutrient concentration showed no significant change relative to SST and Chlor-*a*, with a range of 0.001 – 8.951mmol/ m^3. While Chlor-a and nitrate concentrations increased, they remained relatively low compared to general standards. This low concentration can be attributed to the influence of the positive Indian Ocean Dipole (IOD) during this period.

The Milky Sea area exhibited high nanoplankton concentrations, ranging from 0.02 to 0.64mg/ m^3, which correlated with lower SST and higher Chlor-a concentrations. SST and Chlor-a levels influence the abundance of nutrients and nanoplankton in these waters.

Based on these parameters, from July 31st to August 4th, 2019, the Milky Sea phenomenon could be identified, characterized by a decrease in SST and an increase in Chlor-*a* and nanoplankton levels, with no significant changes in nutrient concentration. Among these factors, SST was the most influential, though other oceanographic conditions also played a role in signaling the potential occurrence of the Milky Sea phenomenon in the southern waters of Java.

ACKNOWLEDGEMENTS

The authors express their gratitude to Universitas Padjadjaran and KomitmenX Research Group for their support in this research. Also thanks to all the committee members of the International Seminar of Indonesian Seas: Catalyst for Ocean Sustainability (ISCO) 2024, who have facilitated the publication process of this manuscript until it was published in the Egyptian Journal of Aquatic Biology and Fisheries.

REFERENCES

Ahmad, A. L.; Syamsuddin, M. L.; Purba, N. P. and Sunarto. (2019). Thermal front condition through El Niño and Indonesian throughflow phase in southern sea of East Java and Bali on the east monsoon. IOP Conf. Ser. Earth Environ. Sci., 303(1). https://doi.org/10.1088/1755-1315/303/1/012002

Amalia, R. H. T.; Tasya, A. K. and Ramadhani, D. (2021). Kandungan Nitrit dan

Nitrat Pada Kualitas Air Permukaan. Pros. Semin. Nas. Biol., 1, 679–688.

Arizuna, M.; Suprapto, D. and Muskananfola, M. R. (2014). Nitrate and Phosphate Content in Sediment Pore Water in the River and Estuary of the Wangun Demak River. Diponegoro J. Maquares, 3(1), 7–16.

Atmadipoera, A. S.; Jasmine, A. S.; Purba, M. and Kuswardani, A. R. T. D. (2020). Upwelling Characteristics in the Southern Java Waters During Strong La Nina 2010 and Super El Nino 2015. J. Ilmu Dan Teknol. Kelaut. Trop., 12(1), 257–276. https://doi.org/10.29244/jitkt.v12i1.28977

Auer, G.; De Vleeschouwer, D.; Smith, R. A.; Bogus, K.; Groeneveld, J.; Grunert, P.; Castañeda, I. S.; Petrick, B.; Christensen, B.; Fulthorpe, C.; Gallagher, S. J. and Henderiks, J. (2019). Timing and Pacing of Indonesian Throughflow Restriction and Its Connection to Late Pliocene Climate Shifts. Paleoceanogr. Paleoclimatology, 34(4), 635–657. https://doi.org/10.1029/2018PA003512

Böttjer, D. and Morales, C. E. (2007). Nanoplanktonic assemblages in the upwelling area off Concepción (∼36°S), central Chile: Abundance, biomass, and grazing potential during the annual cycle. Prog. Oceanogr., 75(3), 415–434. https://doi.org/https://doi.org/10.1016/j.pocean.2007.08.024

Das, N. and Pandey, A. (2015). Role of Nanoplanktons in Marine Food-Webs. Int. Lett. Nat. Sci., 43(November), 38–47. https://doi.org/10.18052/www.scipress.com/ilns.43.38

E.U.Copernicus Marine Service Information (CMEMS). (2023). *Global Ocean Colour and Reflectances MY L3*.

E.U Copernicus Marine Service Information (CMEMS). (2023). *Global Ocean Biogeochemistry Hindcast*. Marine Data Store (MDS). https://doi.org/https://doi.org/10.48670/moi-00019

ERDDAP (2023). *Near Real Time Geostrophic Currents*.

Fischer, A. D.; Hayashi, K.; McGaraghan, A. and Kudela, R. M. (2020). Return of the "age of dinoflagellates" in Monterey Bay: Drivers of dinoflagellate dominance examined using automated imaging flow cytometry and long-term time series analysis. Limnol. Oceanogr., 65(9), 2125–2141. https://doi.org/10.1002/lno.11443

Hackett, J. D.; Anderson, D. M.; Erdner, D. L. and Bhattacharya, D. (2004). Dinoflagellates: A remarkable evolutionary experiment. Am. J. Bot., 91(10), 1523–1534. https://doi.org/10.3732/ajb.91.10.1523

Haddock, S. H. D.; Moline, M. A., and Case, J. F. (2010). Bioluminescence in the Sea. *Annual Review of Marine Science*, *2*(2), 443–493. https://doi.org/https://doi.org/10.1146/annurev-marine-120308-081028

Haryanto, Y. D.; Riama, N. F.; Agdialta, R. and Hartoko, A. (2021). Sea Surface Temperature (SST) analysis during ElNio-LaNia in the Java Sea. IOP Conf. Ser. Earth Environ. Sci., 716(1). https://doi.org/10.1088/1755-1315/716/1/012006

Herwindya, A. Y.; Soepardjo, A. H. and Aldrian, E. (2018). The effect of the Pacific

Ocean water mass on water and climate around Maluku. AIP Conf. Proc., 2023(January). https://doi.org/10.1063/1.5064200

Hirata, T.; Hardman-Mountford, N. J.; Brewin, R. J. W.; Aiken, J.; Barlow, R.; Suzuki, K.; Isada, T.; Howell, E.; Hashioka, T.; Noguchi-Aita, M. and Yamanaka, Y. (2011). Synoptic relationships between surface Chlorophyll-a and diagnostic pigments specific to phytoplankton functional types. Biogeosciences, 8(2), 311–327. https://doi.org/10.5194/bg-8-311-2011

Khan, A. M. A.; Ilmi, M. H.; Febriani, C.; Sidik, T. D. A.; Azizah, F. N.; Ramadhanti, D. S. and Purba, N. P. (2024). Variability of biophysical parameters during La Niña condition in the Eastern Region of the Indian Ocean. J. Sea Res., 201(August), 102533. https://doi.org/10.1016/j.seares.2024.102533

Kunarso; Safwan, H.; Nining, N. S. and Mulyono, B. S. (2011). Variabilitas Suhu dan Klorofil-a di Daerah Upwelling pada Variasi Kejadian ENSO dan IOD di Perairan Selatan Jawa sampai Timor. Indones. J. Mar. Sci., 16(3), 171–180.

Mesinger, A. F. and Case, J. F. (1992). Dinoflagellate luminescence increases susceptibility of zooplankton to teleost predation. Mar. Biol., 112(2), 207–210. https://doi.org/10.1007/BF00702463

Miller, S. D. (2022). Boat encounter with the 2019 Java bioluminescent milky sea: Views from on-deck confirm satellite detection. In R. Dickinson (Ed.), Proceedings of the National Academy of Sciences of the United States of America (Vol. 119, Issue 29, pp. 1–3). https://doi.org/10.1073/pnas.2207612119

Miller, S. D.; Haddock, S. H. D.; Elvidge, C. D. and Lee, T. F. (2005). Detection of a bioluminescent milky sea from space. Proc. Natl. Acad. Sci. U. S. A., 102(40), 14181–14184. https://doi.org/10.1073/pnas.0507253102

Miller, S. D.; Haddock, S. H. D.; Elvidge, C. D. and Lee, T. F. (2006). Twenty thousand leagues over the seas: The first satellite perspective on bioluminescent "milky seas." Int. J. Remote Sens., 27(23), 5131–5143. https://doi.org/10.1080/01431160600554298

Miller, S. D.; Haddock, S. H. D.; Straka, W. C.; Seaman, C. J.; Combs, C. L.; Wang, M.; Shi, W. and Nam, S. H. (2021). Honing in on bioluminescent milky seas from space. Sci. Rep., 11(1), 1–10. https://doi.org/10.1038/s41598-021-94823-z

NASA Ocean Biology Processing Group. (2024). *Aqua-MODIS Chlorophyll Concentration Level-2 Ocean Color Data*. Ocean Color. https://oceancolor.gsfc.nasa.gov/l3/

Naulita, Y.; Arhatin, R. E. and Nabil. (2020). Upwelling index along the South Coast of Java from satellite imagery of wind stress and sea surface temperature. IOP Conf. Ser. Earth Environ. Sci., 429(1). https://doi.org/10.1088/1755-1315/429/1/012025

Neliyana, A.; Wiryawan, B.; Wiyono, E. S. and Nurani, T. W. (2016). Analysis Financial Fisheries of Purse Seine in Lampulo Fishing Port Banda Aceh Provinsi

Aceh. Mar. Fish. J. Mar. Fish. Technol. Manag., 5(2), 163–169. https://doi.org/10.29244/jmf.5.2.163-169

Ocean Data View. (2003). *Ocean Data View User ' s Guide*.

Paringgi (2019). Data pasang surut air laut tahun 2019. BPBD PANGKALPINANG.

Patty, S. I. (2015). Karakteristik Fosfat, Nitrat dan Oksigen Terlarut di Perairan Selat Lembeh, Sulawesi Utara. J. Pesisir Dan Laut Trop., 3(2), 1. https://doi.org/10.35800/jplt.3.2.2015.9581

Pitcher, G. C.; Boyd, A. J.; Horstman, D. A. and Mitchell-Innes, B. A. (1998). Subsurface dinoflagellate populations, frontal blooms and the formation of red tide in the southern Benguela upwelling system. Mar. Ecol. Prog. Ser., 172, 253–264. https://doi.org/10.3354/meps172253

Pranowo, W. S.; Tussadiah, A.; Syamsuddin, M. L.; Purba, N. P. and Riyantini, I. (2016). Karakteristik dan Variabilitas Eddy di Samudera Hindia Selatan. Segara, 12(3), 129–137. https://doi.org/10.15578/segara.v12i3.121

Pratiwi, D. P.; Nurrachmi, I. and Thamrin. (2015). The Relations Between the Concentration of Nitrate and Phosphate to Abundance of Dinoflagellates in Enhalus acoroides Beds in Sungai Enam Coastal Waters of Bintan Regency of Riau Islands Province. J. Online Mhs., 26(3), 1–5.

Purba, N. P. and Khan, A. M. A. (2019). Upwelling Session in Indonesia Waters. World News Nat. Sci., 25(June), 72–83.

Purba, N. P.; Pranowo, W. S.; Faizal, I. and Adiwira, H. (2018). Temperature-Salinity stratification in the Eastern Indian Ocean using argo float. IOP Conf. Ser. Earth Environ. Sci., 162(1), 1–10. https://doi.org/10.1088/1755-1315/162/1/012010

Purba, N. P.; Pranowo, W. S.; Ndah, A. B. and Nanlohy, P. (2021). Seasonal variability of temperature, salinity, and surface currents at 0° latitude section of Indonesia seas. Reg. Stud. Mar. Sci., 44(101772). https://doi.org/https://doi.org/10.1016/j.rsma.2021.101772.

Purba, N. P.; Akhir, M. F.; Faid, G. M.; Roseli, N. H.; Sinaga, I. F. and Faizal, I. (2025). Stratified Ocean Chlorophyll-a and Nutrient Availability in the Eastern Tropical Indian Ocean during La Nina 2022-2023. Egypt. J. Aquat. Biol. Fish., 29(1), 297–320. https://journals.ekb.eg/article_404325_65eaf9435686a2eb43aa9a68258ed2f0.pdf

Qasim, S. Z. (1999). Some Unique Characteristics of The Indian Ocean. Qatar Univ. Sci. J., 19, 111–116. https://doi.org/http://hdl.handle.net/10576/9788

Rasyid J, A. (2016). Distribution of Chlorophyll-a in The Season of East in Spermonde Aquatic South Sulawesi. Fish Sci., 1(2), 105–116.

Ratna, S. B.; Cherchi, A.; Osborn, T. J.; Joshi, M. and Uppara, U. (2021). The Extreme Positive Indian Ocean Dipole of 2019 and Associated Indian Summer Monsoon Rainfall Response. Geophys. Res. Lett., 48(2), 1–11. https://doi.org/10.1029/2020GL091497

Rosel, P. and Mullin, K. (2011). Photoidentification capture-mark-recapture techniques

for estimating abundance of bay, sound and estuary populations of bottlenose dolphins along the US. NOAA Tech.

Sabhan, S.; Pranowo, W. S.; Purba, M. andKoropitan, A. F. (2020). Model Perpindahan Vertikal Massa Air Oleh Interaksi Arus Dan Topografi Di Teluk Palu. Positron, 10(1), 42. https://doi.org/10.26418/positron.v10i1.37263

Saji, N. H.; Goswami, B. N.; Vinayachandran, P. N. and Yamagata, T. (1999). A Dipole Mode in The Tropical Indian Ocean. Nature, 401, 360–363. https://doi.org/https://doi.org/10.1038/43854

Sardessai, S.; Shetye, S.; Maya, M. V.; Mangala, K. R. and Prasanna Kumar, S. (2010). Nutrient characteristics of the water masses and their seasonal variability in the eastern equatorial Indian Ocean. Mar. Environ. Res., 70(3–4), 272–282. https://doi.org/10.1016/j.marenvres.2010.05.009

Serodja, C. M.; Ismanto, A.; Hakim, A. R. and Ramdhani, A. (2023). Analisa Pengaruh Angin Monsoon Timur terhadap Arus Permukaan Berdasarkan Data HF Radar di Perairan Selat Sunda. Indones. J. Oceanogr., 4(4), 11–18. https://doi.org/10.14710/ijoce.v4i4.15672

Setiawan, A.; Noor, G. E.; Trenggono, M.; Putri, M. R.; Agustiadi, T.; Priyono, B.; Yu, W. and Wang, H. (2015). Analysis of Java Upwelling in the Indian Ocean Southwest of Java Based on the Stability of Water Mass. Conf. 12th Annu. Meet. Asia Ocean. Geosci. Soc.

Sofiati, I.; Yulihastin, E. and Putranto, M. F. (2020). Meridional variations of sea surface temperature and wind over southern sea of Java and its surroundings. J. Phys. Its Appl., 3(1), 129–135. https://ejournal2.undip.ac.id/index.php/jpa/index

Sumantra, I. G. E.; Suteja, Y. and Putra, I. N. G. (2020). Fluktuasi Nitrat dan Fosfat Selama Satu Periode Pasang dan Surut di Selat Lombok. J. Mar. Aquat. Sci., 6(2), 231. https://doi.org/10.24843/jmas.2020.v06.i02.p10

Trainer, V. .;LHickey, B. M.; Lessard, E. J.; Cochlan, W. P.; Trick, C. G.; Wells, M. L.; MacFadyen, A. and Moore, S. K. (2009). Variability of Pseudo-nitzschia and domoic acid in the Juan de Fuca eddy region and its adjacent shelves. Limnol. Oceanogr., 54(1), 289–308. https://doi.org/10.4319/lo.2009.54.1.0289

Valiadi, M. and Iglesias-Rodriguez, D. (2013). Understanding bioluminescence in dinoflagellates—how far have we come? Microorganisms, 1(1), 3–25. https://doi.org/10.3390/microorganisms1010003

Varela, R.; Santos, F.; Gómez-Gesteira, M.; Álvarez, I.; Costoya, X. and Días, J. . (2016). Influence of Coastal Upwelling on SST Trends along the South Coast of Java. PLoS One, 11(9). https://doi.org/https://doi.org/10.1371/journal.pone.0162122

Wang, G.; Cai, W.; Yang, K.; Santoso, A. and Yamagata, T. (2020). A Unique Feature of the 2019 Extreme Positive Indian Ocean Dipole Event. Geophys. Res. Lett., 47(18), 1–9. https://doi.org/10.1029/2020GL088615

Wei, X.; Liao, X.; Zhan, H. and Liu, H. (2012). Estimates of potential new production in the Java-Sumatra upwelling system. Chinese J. Oceanol. Limnol., 30(6), 1063–1067. https://doi.org/10.1007/s00343-012-1281-x

Wibowo, A. (2021). *Modeling the underlying environmental factors of milky sea case and luminous bacteria presence in Java Southern Sea in 2019.* https://doi.org/10.1101/2021.09.10.459852

Wisetya Dewi, Y.; Wirasatriya, A.; Nugroho Sugianto, D.; Helmi, M.; Marwoto, J. and Maslukah, L. (2020). Effect of ENSO and IOD on the Variability of Sea Surface Temperature (SST) in Java Sea. IOP Conf. Ser. Earth Environ. Sci., 530(1). https://doi.org/10.1088/1755-1315/530/1/012007

Wyrtki, K. (1962). The upwelling in the region between java and Australia during the south-east monsoon. Mar. Freshw. Res., 13(3), 217–225. https://doi.org/10.1071/MF9620217

Yan, W.; Chen, Z.; Zhang, L.; Wang, F.; Zhang, G. and Sun, J. (2023). Nanophytoplankton and microphytoplankton in the western tropical Pacific Ocean: its community structure, cell size and carbon biomass. Front. Mar. Sci., 10(April), 1–14. https://doi.org/10.3389/fmars.2023.1147271

Zainuddin, M.; Safruddin, S.; Selamat, M. B.; Farhum, A. and Hidayat, S. (2017). Prediction of Potential Fishing Zones for Skipjack Tuna During the Northwest Monsoon Using Remotely Sensed Satellite Data. ILMU Kelaut. Indones. J. Mar. Sci., 22(2), 59–66. https://doi.org/10.14710/ik.ijms.22.2.59-66